The 9th IEEE International Conference on Intelligent Data Acquisition and Advanced Computing Systems: Technology and Applications
21-23 September, 2017, Bucharest, Romania

Skin Lesions Dermatological Shape Asymmetry Measures

Piotr Milczarski, Zofia Stawska, Paweł Maślanka
Faculty of Physics and Applied Informatics, University of Lodz, Pomorska str. 149/153, Lodz, Poland
{piotr.milczarski,zofia.stawska,pmaslan}@uni.lodz.pl, http://wfis.uni.lodz.pl

***Abstract*—The paper presents deriving of shape asymmetry measure in the dermatological sense (*DASMShape*). The skin lesion symmetry consists of three factors: shape, hue/color and structure. We analyze the shape asymmetry and on its basis we propose a new asymmetry degree realized in several ways. DASMShape methods verification and comparison is performed using PH2 database. The results received after optimization of the DASMShape algorithm are tested on PH2 dataset and discussion about their accuracy is provided. These results shows bigger overestimation than underestimation tendency results. DASMShape measure and its results are the initial points to derive dermatological asymmetry measure.**

Keywords—dermatological shape asymmetry measure; dermatological features; skin lesions rating;

I. INTRODUCTION

Malignant melanoma is the most deadly form of skin cancer. Expert systems supporting diagnostic, especially for non-specialist, are very important in detection early stage of disease [1][19][24]. To properly diagnose a skin lesion, an appropriate algorithms measuring various disease aspects is necessary. It was assumed that 3-point checklist (3PCLD) [19][24] is sufficient to avoid melanoma unrecognition [1] or misclassification.

The 3-point checklist [19][24] methodology uses a simple model of the lesion characteristics assessment. This is a method designed for non-dermatologists to detect suspicious skin lesions that may be malignant. It is reported [1] that the effectiveness of malignancy recognition by non-dermatologists using this method is about 96%, although the diagnosis of a specific disease is only about 32%.

The conclusion drawn from the dermatologists experts researches presented above is that the non-experts, that are usually general practitioners, need a proper support. One of such a solutions can be an automated expert system that could support the diagnosis [2][25]. That is the reason why we concentrate on the automated lesion detection and defining their characteristic features [15][21]. There is a need for a system that automatically recognizes the features of lesion taken into account by doctors using a 3-point checklist.

The paper is divided into five sections. The next section presents the steps that such a system must perform to properly classify a lesions and their features. The dermoscopic database PH2 is also shortly described. Dermatological Asymmetry Measure (DASM) is shown in Section III. Section IV presents two Dermatological Asymmetry Measures of Shape (DASMShape). The discussion of the two measures as well as the conclusions are drawn in Section V.

II. SKIN LESIONS RECOGNITION SCHEME

To perform a final prediction computer-aided diagnostic system should have three steps [9][15][21][22]:

The first step is the lesion borders segmentation [5][18][23].

The second essential **step** is clinical feature segmentation [3][4]. The result of this step is a binary mask of clinical attributes.

The **final** classification (**the third step**) is relying on the appliance of optimal recognition method considering the previous steps and patient medical interview [6][7][8][10][17].

Segmentation of the objects that stand out from the background by their color or texture is a common problem and there are a whole range of solutions that can be applied in this case [5][13][18][23]. However, the specificity of this problem should be taken into account in order to select e.g. the appropriate functions to detect skin areas [5][10] as well as to eliminate the differences between images resulting e.g. from the patient's skin color or lesion arrangement [14][20].

In the process of clinical features segmentation we look for characteristics typical for the melanoma e.g. irregular shape, atypical pigment network, blue-whitish veil, depigmentation, globules and dots [1][3][4][21]. The clinical feature segmentation can use various attributes as hue/color, texture, structure, shape, location [24]. The feature structure can be categorized by their different patterns [3][22].

In the paper, the authors study concerning one of the features characterizing atypical skin lesions, namely lesion shape asymmetry is described. To verify the results, as a reference database we used the PH2 database [11]. PH2 consists of 200 dermoscopic images described by expert dermatologists, derived into 3 groups: common lesion, atypical lesion and melanoma (80/80/40 cases correspondingly). Each described case contains shape of

the lesion gained in manual segmentation, clinical diagnosis and set of features collected by experts. Dermoscopic color images, acquired all in the same conditions, have resolution approximately 768x560 pixels.

Diagnosis of the lesions requires an algorithms detecting disease changes. There are several known methods used by dermatologists: ABCD or ABCDE rule, three-point or seven-point checklist [1]. The expanded version of 3-point checklist are CASH algorithm [12] and extended 3PCLD (x3PCLD) [21]. Each of these methods takes into account symmetry/asymmetry of lesions. Symmetry/asymmetry is determined by 3 factors: shape, color and structure. Each of them influences the final evaluation of lesions symmetry or asymmetry. Further in the paper we are referring to symmetry/asymmetry as asymmetry.

In our research we used 3-point checklist, defined as follows [24]:

- Asymmetry: asymmetry of shape, color/hue and/or structure in one or two perpendicular axes;
- Atypical network: pigment network with irregular holes and thick lines;
- Blue-white structures: any type of blue and/or white color, i.e. combination of blue-white veil and regression structures.

If the lesion presents at least two of these criteria, there is a high probability of melanoma [19][24].

Irregularity of lesion is one of the 3 decisive evaluation criteria in a 3-point checklist [19]. It consists of 3 factors: shape, hue/color and structure. Each of them may have its own asymmetry. To obtain reliable information about the asymmetry of the lesion, we need to consider each of these factors separately. The first step in our work is to evaluate the asymmetry of the shape of the lesion. The result of this evaluation will become a component of the final diagnosis of the irregularity of skin lesions.

III. Dermatological Asymmetry Measure, DASM

In the introduced Dermatological Asymmetry Measure (DASM) [15] the combination of 3 factors (shape, hue, structure) was defined as asymmetry measure. There have been also introduced separate measures of shape (DASMShape), hue/color distribution (DASMHue) and structure distribution (DASMStruct) with their continuous values from the subset <0,2>. In the future, the DASM measure will consist of the above asymmetry measures of all three elements.

In our reference database (PH2) the following symmetry values were adopted:

0 – symmetrical lesion in two perpendicular axes;

1 – lesion symmetrical in one axis (partial symmetry);

2 – asymmetrical lesion.

Based on the same indications, we proposed a more precise definition of the value of symmetry in continuous form. All three values that make up the final evaluation of the symmetry of lesion (shape, color and structure) can assume continuous values from the range of <0,2> to be consistent with the values used by dermatologists and defined above.

In this work we present only the method of determining the value of the shape asymmetry.

IV. Dermatological Asymmetry Measure of Shape, DASMShape

As a result of the lesion image segmentation, we receive a binary mask corresponding to the lesion. It will be the basis for defining the lesion asymmetry [18]. Further in the section, we propose a new measure to determine the degree of asymmetry. In order to preserve the maximum knowledge of lesion shape we decided to describe asymmetry as a real number from the range <0.2>.

In the paper, apart from the definitions and abbreviations defined above the following definitions and abbreviations are defined:

- DAS – Dermatological Asymmetry, value of asymmetry of the shape, hue and structure assigned by dermatologists (0, 1 or 2)
- DASM – Dermatological Asymmetry Measure It depends on DASMShape, DASMHue and DASMStruct
- GSSPT – a geometrical shape symmetry precision threshold.
- NSA – number of symmetry axes depending on GSSPT.
- VoSS – a vector of shape symmetry. Its coefficients are equal to the NSA
- GCL – a geometric center of the lesion.
- LSA – list of symmetry axes

The starting point of the method of deriving and calculating DASMShape value is binary mask achieved after segmentation. The value of the dermatological asymmetry (DAS) for four examples of binary masks are shown in Fig. 1. These are the values attributed to lesions by dermatologist experts [11].

To calculate the degree of dermatological asymmetry we use the following algorithm:

1. Derive the number of symmetry axes for every threshold t_i from a set of GSSPT thresholds $n(t_i)$,.Taking into account our experimental calculations we propose the thresholds' values as a subset of a set of the values below:

   $\{0.9, 0.91, 0.92, 0.93, 0.94, 0.95, 0.96, 0.97, 0.98\}$.

2. Construct a vector of shape symmetry (VoSS) **W** from the $n(t_i)$ values:

   $$W = [n(t_1), n(t_2), ..., n(t_k)], \quad (1)$$

   where $k \geq 2$.
3. Define the function *DASMShape*, as a function of shape symmetry vector VoSS. That function should be normalized to real values from the

subset <0,2>. In the paper, two types of functions normalized to maximum value of 2 are presented and discussed.

a. The first one, an exponential type of vector **W**:

$$DASMShape(W) = 2\exp(-f(W)) \quad (2)$$

where f: $R^k \rightarrow R^+ \cup \{0\}$.

b. The second type defined as rational one depending on a vector **W**:

$$DASMShape(W) = \frac{2}{f(W)} \quad (3)$$

where inner function f: $R^k \rightarrow <1, \infty)$.

For each of the DASMShape functions let us introduce a set of two crisp shape thresholds (ST): ST={lst, ust}, where

$$ST(DASMShape(W)) = \begin{cases} 0 \Leftrightarrow DASMShape(W) < lst \\ 1 \Leftrightarrow lst \le DASMShape(W) < ust \\ 2 \Leftrightarrow DASMShape(W) > ust \end{cases} \quad (4)$$

The values of *lst* and *ust* will depend on the DASMShape function type and will be derived after optimization of results. The number of misclassified images should have minimum value parallely with the number of underestimated cases.

V. Results and Conclusions

Dermatological symmetry is not a symmetry in the mathematical sense. We could say that it is "inaccurate symmetry". The main problem of the constructing a measure of the dermatological symmetry is finding satisfactory parameters that the symmetry is sufficient but not too accurate. The verification of our measures is based on expert assessments contained in the PH2 database. We have chosen a set of binary masks in Figures 2a-2d to present different values of the DASMShape and dermatological measure DAS.

In our research, several versions of function f **(W)** in (2) and (3) with different coefficients and for a different subset of GSSPT thresholds have been tested. The time and resources, demanded for deriving of VoSS vector **W,** are proportional to the number of thresholds t_i**.** We have obtained the best results for the subset of threshold values:

$$\{0.9, 0.93, 0.94, 0.95, 0.97\} . \quad (4)$$

It has to be taken into account that the bigger threshold the more accurate the shape should be acquired to achieve the best asymmetry value.

The tests were conducted using proprietary java program run on processor Intel® Core™ i7-4900MQ CPU @ 2.80GHz, 2801 MHz, Cores: 4, Logical processors: 8. The images from PH2 dataset have 768x560 resolution as well as the binary masks used to determine the symmetry/asymmetry axes. The average time to derive the DASMShape of the lesion and their possible axes varied from 0.8 sec to 2.03 sec.

A. Exponential Type of DASMShape

In the exponential case of the DASMShape, we propose to define the inner function f**(W)** as follows:

$$f(W) = \sum_{i=5}^{5} a_i n_i^2 \quad (5)$$

where the values $n=n(t)$ defined for the thresholds in (4) are $n_1 = n(t_1) = n(0.9), \ldots, n_5 = n(t_5) = n(0.95)$.

In the research, we have tested several vectors of coefficients **a:**

$$\mathbf{a}=[a_1, \ldots, a_5] . \quad (6)$$

We present 3 examples of them. They are labelled as $\mathbf{a_x}$, $\mathbf{a_y}$, $\mathbf{a_z}$ with coefficient shown below

$$\mathbf{a_x} = [0.01, 0.025, 1/15, 1/3, 1.0] \quad (7)$$
$$\mathbf{a_y} = [0.01, 0.02, 0.04, 0.2, 2.0] \quad (8)$$
$$\mathbf{a_z} = [0.004, 0.01, 1/6, 1/3, 0.5] \quad (9)$$

B. Rational Type of DASMShape

In the rational case of the DASMShape, we propose to define the inner function f**(W)** as follows:

$$f(W) = 1 + \sum_{i=5}^{5} a_i n_i \quad (10)$$

where the values $n=n(t)$ defined for the thresholds in (4) are $n_1 = n(t_1) = n(0.9), \ldots, n_5 = n(t_5) = n(0.95)$.

If the thresholds' values are all equal 0, then f(W) value equals 1. Hence, the DASMShape function defined as in (3) has no singularity and the set of values is (0,2> as well as the corresponding set for that function defined as in (2).

In the research, we have tested several vectors of coefficients **a** for a rational DASMShape measure (3), (10)**.** We present 2 examples of them. They are labelled as $\mathbf{a_k}$ and $\mathbf{a_m}$, with coefficient presented below:

$$\mathbf{a_k} = [0.004, 0.01, 0.17, 0.33, 0.5] \quad (11)$$
$$\mathbf{a_m} = [0.1, 0.2, 0.3, 0.5, 0.9] \quad (12)$$

TABLE I. THE EXAMPLES OF VOSS VECTOR **W** FOR SELECTED IMAGES FROM PH2 [11] DATASET

Image ID from PH2	VoSS vector W coefficient values					*DAS* (PH2)	DASMShape values for f(W) and coefficients a				
	n(0.9)	*n*(0.93)	*n*(0.94)	*n*(0.95)	*n*(0.97)		a_x	a_y	a_z	a_k	a_m
IMD003	10	4	3	0	0	**0**	0.27067	0.37275	0.25491	1.43885	0.54054
IMD035	1	0	0	0	0	**2**	1.98010	1.98010	1.99202	1.99800	1.81818
IMD002	8	3	3	1	0	**1**	0.33115	0.50316	0.22623	1.13122	0.52632
IMD075	1	1	1	0	0	**2**	1.80666	1.86479	1.66943	1.78412	1.25000
IMD155	2	2	2	2	1	**0**	0.12914	0.09192	0.15523	0.53447	0.39216
IMD339	12	12	7	6	0	**2**	0.00000	0.00000	0.00000	0.12231	0.08097
IMD211	2	1	1	1	0	**1**	1.25627	1.48164	1.18193	1.31406	0.90909
IMD405	2	1	1	1	0	**2**	1.25627	1.48164	1.18193	1.31406	0.90909
IMD406	13	6	5	2	0	**2**	0.00747	0.02969	0.00290	0.61862	0.28571

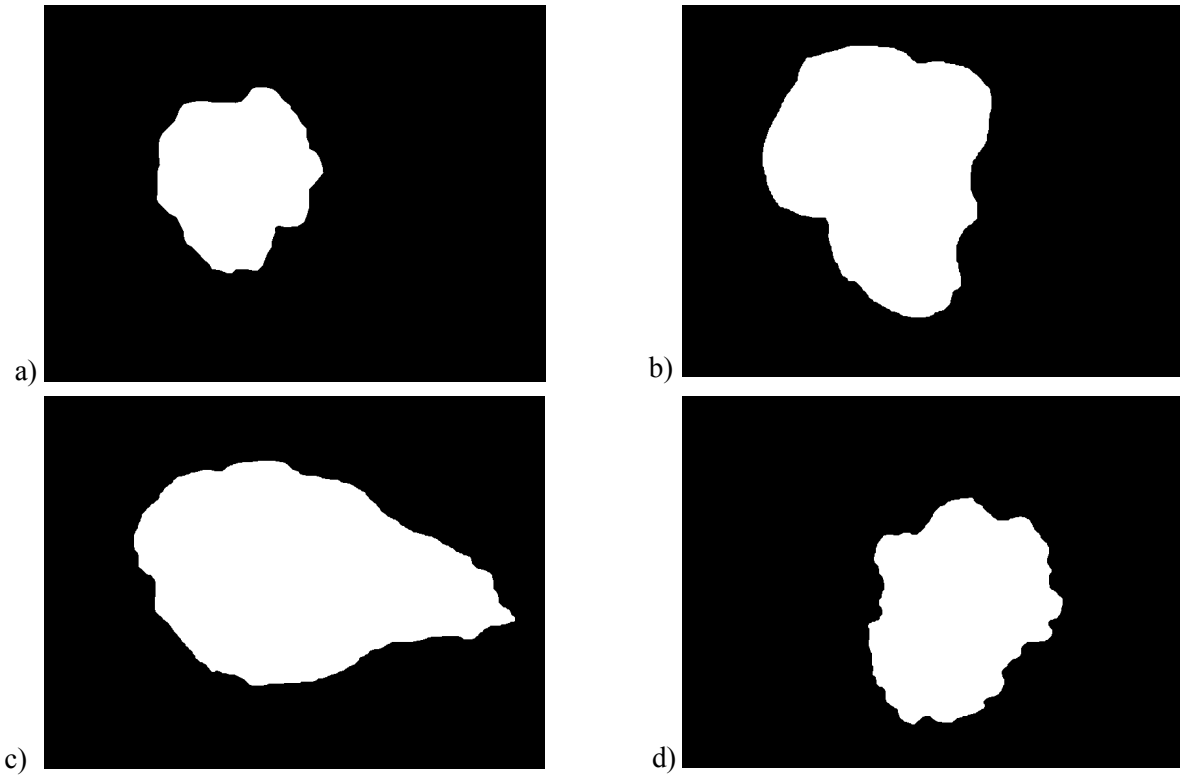

Figure 1. The examples of PH2 dataset binary images [11] with the values of dermatological asymmetry DAS. a) IMD003 (Common nevus) DAS=0; b) IMD075 (Atypical nevus) DAS=2; c) IMD211 (Nodular Melanoma) DAS=1; d) IMD405 (Nodular Melanoma) DAS= 2

The VoSS vectors **W** are presented in Tab. I for selected images. In the last right columns, there are shown values of the function $f(\mathbf{W})$ defined above in (5) and (10) with the coefficients as in (7)-(9) and (11) and (12) with 5 digit accuracy.

Table I shows also that some of the results and values of DASMShape and DAS disagree with each other.

PH2 dataset contains around 33 images containing part of the lesion. In that cases shape symmetry/asymmetry cannot be calculated properly. Hence, in Tables II-VIII the classification results for 167 images are shown (out of 200).

TABLE II. RESULTS OF CLASSIFICATION FOR PH2 DATASET, FOR EXPONENTIAL TYPE ST= {1.119,1.45} AND $\mathbf{A=A_X}$

DAS value PH2	Number of images with DAS	No. of misclassified images DASMShape				
		0	**1**	**2**	**No. of misclassified**	**Overestimated**
0	107	-	9	19	28	36
1	31	14	-	8	22	
2	29	7	4	-	11	
Total	167	21	13	27	61	
Underestimated		25				**$a=a_x$**

TABLE III. RESULTS OF CLASSIFICATION FOR PH2 DATASET, FOR EXPONENTIAL TYPE ST= {1.098,1.41} AND $\mathbf{A=A_Y}$

DAS value PH2	Number of images with DAS	No. of misclassified images DASMShape				
		0	1	2	No. of misclassified	Overestimated
0	107	-	15	23	38	50
1	31	12	-	12	24	
2	29	5	3	-	8	
Total	167	17	18	35	70	
Underestimated		20				$\mathbf{a=a_y}$

TABLE IV. RESULTS OF CLASSIFICATION FOR PH2 DATASET, FOR EXPONENTIAL TYPE ST= {0.971,1.532} AND $\mathbf{A=A_Z}$

DAS value PH2	Number of images with DAS	No. of misclassified images DASMShape				
		0	1	2	No. of misclassified	Overestimated
0	107	-	13	21	34	42
1	31	11	-	8	19	
2	29	6	5	-	11	
Total	167	17	18	29	64	
Underestimated		22				$\mathbf{a=a_z}$

TABLE V. RESULTS OF CLASSIFICATION FOR PH2 DATASET, FOR EXPONENTIAL TYPE ST= {1.096,1.527} AND $\mathbf{A=A_Z}$

DAS value PH2	Number of images with DAS	No. of misclassified images DASMShape				
		0	1	2	No. of misclassified	Overestimated
0	107	-	11	21	32	40
1	31	12	-	8	20	
2	29	7	4	-	11	
Total	167	19	15	29	63	
Underestimated		23				$\mathbf{a=a_z}$

Total numbers of images with a given DAS value for 167 full lesion images from PH2 dataset are: 107 images with DAS=0, 31 images with DAS=1 and 29 images with DAS=2.

In the Tables IV and V, there are shown two exemplary tables with the same inner DASMShape function $\mathbf{a=a_z}$ but with a different set of ST thresholds:

- ST= {0.971,1.532} with 22 underestimated and 64 misclassified cases ;
- ST= {1.096,1.527} with 23 underestimated and 64 misclassified cases.

As it can be seen from the above examples the results in Tab. IV are better or more promising because they have less underestimated cases. The second pointer is that the underestimation in asymmetric cases (with DAS=2) shows that that totally asymmetric cases are classified closer to the expert judgement (closer to DAS).

The similar discussion like for Tables IV and V can be done for the results from the Tables VII and VIII. With different upper thresholds the number of underestimated cases fifer by 1 but the number of misclassified asymmetrical ones (DAS=2) is lower by 2. That is why we take into account later classifier shown in Tab. VIII.

TABLE VI. RESULTS OF CLASSIFICATION FOR PH2 DATASET, FOR RATIONAL TYPE ST= {0.79,1.31} AND $\mathbf{A=A_K}$

DAS value PH2	Number of images with DAS	No. of misclassified images DASMShape				
		0	1	2	No. of misclassified	Overestimated
0	107	-	30	33	63	81
1	31	7	-	18	25	
2	29	4	2	-	6	
Total	167	11	32	51	94	
Underestimated		13				$\mathbf{a=a_k}$

TABLE VII. RESULTS OF CLASSIFICATION FOR PH2 DATASET, FOR RATIONAL TYPE ST= {0.801, 1.15} AND $\mathbf{A=A_M}$

DAS value PH2	Number of images with DAS	No. of misclassified images DASMShape				
		0	1	2	No. of misclassified	Overestimated
0	107	-	15	14	29	36
1	31	13	-	7	20	
2	29	7	6	-	13	
Total	167	20	21	21	66	
Underestimated		26				$\mathbf{a=a_m}$

TABLE VIII. RESULTS OF CLASSIFICATION FOR PH2 DATASET, FOR RATIONAL TYPE ST= {0.801, 1.045} AND $\mathbf{A=A_M}$

DAS value PH2	Number of images with DAS	No. of misclassified images DASMShape				
		0	1	2	No. of misclassified	Overestimated
0	107	-	10	19	29	37
1	31	13	-	8	21	
2	29	7	4	-	11	
Total	167	20	14	27	61	
Underestimated		24				$\mathbf{a=a_m}$

Even if the DASMShape inner functions have the same structure and order the results might differ e.g. because the ST thresholds and the inner function coefficients like in cases shown in Tables VI-VIII.

The results shown in Tab. VI point that the rational type of DASMShape function with $\mathbf{a=a_k}$ as a satisfactory classifier cannot be taken into account in comparison with the results given by the $\mathbf{a_x}$,$\mathbf{a_y}$, $\mathbf{a_z}$, and $\mathbf{a_m}$. That case was shown only for the discussion reason.

After optimization of the thresholds values for the coefficients $\mathbf{a_x}$,$\mathbf{a_y}$, $\mathbf{a_z}$, and $\mathbf{a_m}$ we obtained the smallest value of misclassified images for the thresholds with underestimated ones for the thresholds ST shown in Tables II, III, IV and VIII.

The differences between the results given by the presented DASMShape functions and dermatological values (DAS) point that shape asymmetry alone can give us good result. The overall symmetry/asymmetry is relative to symmetry in shape, hue or structure altogether.

The Tables II-VIII show that for 29 cases with DAS=2 DASMShape functions indicates full symmetry in shape.

Comparing the results of the classifiers shown in Tables II, III, IV and VIII we achieved that the DASMShape methods are:

- misclassifying on the same set of 52 cases (18 with DAS=2, 18 with DAS=1, 26 with DAS=0) i.e. IMD003and IMD075 (see Fig. 2);
- classifying correctly on the same set of 90 cases (18 with DAS=2, 5 with DAS=1, 67 with DAS=0) i.e. IMD339 and IMD406 (see Fig. 2).

Apart from estimating shape symmetry/asymmetry of the lesion we achieve also the geometric center of the lesion and the list of the symmetry axes. That list of axes will be a starting point for estimating dermatological asymmetry measure of hue distribution DASMHue [16].

In the future a measure of the asymmetry of hue and structure will be developed. It seems that only the combination of these three qualities can give rise to an assessment of the degree of asymmetry of skin lesion.

The proposed measures should be evaluated in correlation with the measure of hue and structure asymmetry, which will probably allow to choose the best one.

The advantage of all proposed measures is their continuity, which allows for a more accurate assessment of the lesion asymmetry degree.

REFERENCES

[1] G. Argenziano, H. P. Soyer, S. Chimenti, R. Talamini, et al. "Dermoscopy of pigmented skin lesions: results of a consensus meeting via the Internet," J*ournal of the American Academy of Dermatology*, vol. 48, no. 9, pp. 679-693, 2003.

[2] C. Barata, M. Ruela, M. Francisco, T. Mendonça and J. S. Marques, "Two systems for the detection of melanomas in dermoscopy images using texture and color features," *IEEE Systems Journal*, vol. 8, no. 3, pp. 965-979, 2014.

[3] C. Barata, J. S. Marques, and J. Rozeira, "A system for the detection of pigment network in dermoscopy images using directional filters," *IEEE Trans. on Biomedical Eng.*, vol. 10, pp. 2744–2754, 2012.

[4] M. H. Bharati, J. F. MacGregor, "Texture analysis of images using Principal Component Analysis," in *Proceedings of the SPIE – Process Imaging for Automatic Control*, vol. 4188, pp. 27-33, 2001.

[5] F. Bogo, F. Peruch, A. B. Fortina and E. Peserico, "Where's the lesion? Variability in human and automated segmentation of dermoscopy images of melanocytic skin lesions," in *Dermoscopy Image Analysis*, M. E. Celebi, T. Mendonca and J. S. Marques, Eds., Boca Raton, CRC Press, 2015, pp. 67-96.

[6] M. E. Celebi, H. A. Kingravi, B. Uddin, et al., "A methodological approach to the classification of dermoscopy images," *Computerized Medical Imaging and Graphics*, vol. 31, no. 6, pp. 362-373, 2007.

[7] N. Codella, J. Cai, M. Abedini, R. Garnavi, A. Halpern and J. R. Smith, "Deep learning, sparse coding, and SVM for melanoma recognition in dermoscopy images," in *Machine Learning in Medical Imaging*, Munich, Springer, pp. 118-126, 2015.

[8] F. Ercal, A. Chawla, W. V. Stoecker, H.-C. Lee and R. H. Moss, "Neural network diagnosis of malignant melanoma from color images," *IEEE Transactions on Biomedical Engineering*, vol. 41, no. 9, pp. 837-845, 1994.

[9] R. Gonzalez, *Digital Image Processing*, Pearson Hall, 2008.

[10] M. Kruk, B. Swiderski, S. Osowski, J. Kurek, M. Slowinska, I. Walecka, "Melanoma recognition using extended set of descriptors and classifiers," *J Image Video Proc.*, vol. 2015(1), Article: 43, Dec 2015.

[11] T. Mendonca, P.M. Ferreira, J.S. Marques, et al., "PH2 – A dermoscopic image database for research and benchmarking," in *Proceedings of the 35th International Conference of the IEEE Eng. in Medicine and Biology Society (EMBC)*, Osaka, pp. 5437-5440, 2013.

[12] N. di Meo, G. Stinco, S. Bonin, A. Gatti, S. Trevisini, G. Damiani, S. Vichi, G. Trevisan, "CASH algorithm versus 3-point checklist and its modified version in evaluation of melanocytic pigmented skin lesions: The 4-point checklist," *Journal of Dermatology*, vol. 42, pp. 1-4, 2015.

[13] M. Mete, S. Kockara and K. Aydin, "Fast density-based lesion detection in dermoscopy images," *Computerized Medical Imaging and Graphics*, vol. 35, issue 2, pp. 128-136, 2011.

[14] P. Milczarski, Z. Stawska, "Complex colour detection methods used in skin detection systems," in *ISIM*, vol. 3, no. 1, pp. 40-52, 2014.

[15] P. Milczarski, Z. Stawska, L. Was, S. Wiak, M. Kot, "New dermatological asymmetry measure of skin lesions," *Int. J. of Neural Networks and Adv. Applications*, Prague, pp. 32-38, 2017.

[16] P. Milczarski, "Skin lesion symmetry of hue distribution", in Proceedings of the 9th IEEE International Conference on Intelligent Data Acquisition and Advanced Computing Systems: Technology and Applications, 21-23 September, 2017, Bucharest, Romania, in press.

[17] A. Saez, C. Serrano and B. Acha, "Global pattern classification in dermoscopic images," in *Dermoscopy Image Analysis*, M. E. Celebi, T. Mendonca and J. S. Marques, Eds., Boca Raton, CRC Press, pp. 183-209, 2015.

[18] P. Schmid, "Segmentation of digitized dermatoscopic images by two-dimensional color clustering," *IEEE Transactions on Medical Imaging*, vol. 18, no. 2, pp. 164-171, 1999.

[19] H. P. Soyer, G. Argenziano, I. Zalaudek, R. Corona, F. Sera, R. Talamini, et al., "Three-point checklist of dermoscopy. A new screening method for early detection of melanoma," *Dermatology*, vol. 208, no. 1, pp. 27–31, 2004.

[20] Z. Stawska, P. Milczarski, "Algorithms and methods used in skin and face detection suitable for mobile applications," *ISIM*, vol. 2, issue 3, pp. 227-238, 2013.

[21] L. Was, P. Milczarski, Z. Stawska et al., "Analysis of skin diseases using segmentation and color hue in reference to melanocytic lesions," in *LNCS*, vol. 10245, Springer, pp. 677-689, 2017.

[22] P. Wighton, T. K. Lee, H. Lui, D.I. McLean, M.S. Atkins, "Generalizing common tasks in automated skin lesion diagnosis," *IEEE Trans Inf Technol Biomed.*, vol. 15, pp. 622-629, 2011.

[23] A. Wong, J. Scharcanski and P. Fieguth, "Automatic skin lesion segmentation via iterative stochastic region merging," *IEEE Transactions on Information Technology in Biomedicine*, vol. 15, no. 6, pp. 929-936, 2011.

[24] I. Zalaudek, G. Argenziano, H. P. Soyer, R. Corona et al., "Three-point checklist of dermoscopy: an open internet study", *British J of Dermatology*, vol. 154, no. 3, pp. 431-437, 2006.

[25] Automatic computer-based diagnosis system for dermoscopy images, ADDI, http://www.fc.up.pt/addi.